Journal of proteome research

pubs.acs.org/jpr

Article

COLMAR Lipids Web Server and Ultrahigh-Resolution Methods for Two-Dimensional Nuclear Magnetic Resonance- and Mass Spectrometry-Based Lipidomics

Cheng Wang, István Timári, Bo Zhang, Da-Wei Li, Abigail Leggett, Amal O. Amer, Lei Bruschweiler-Li, Rachel E. Kopec, and Rafael Brüschweiler*

Cite This: *J. Proteome Res.* 2020, 19, 1674–1683

Read Online

ACCESS | Metrics & More | Article Recommendations | Supporting Information

ABSTRACT: Accurate identification of lipids in biological samples is a key step in lipidomics studies. Multidimensional nuclear magnetic resonance (NMR) spectroscopy is a powerful analytical tool for this purpose as it provides comprehensive structural information on lipid composition at atomic resolution. However, the interpretation of NMR spectra of complex lipid mixtures is currently hampered by limited spectral resolution and the absence of a customized lipid NMR database along with user-friendly spectral analysis tools. We introduce a new two-dimensional (2D) NMR metabolite database "COLMAR Lipids" that was specifically curated for hydrophobic metabolites presently containing 501 compounds with accurate experimental 2D ^{13}C-^{1}H heteronuclear single quantum coherence (HSQC) chemical shift data measured in $CDCl_3$. A new module in the public COLMAR suite of NMR web servers was developed for the (semi)automated analysis of complex lipidomics mixtures (http://spin.ccic.osu.edu/index.php/colmarm/index2). To obtain 2D HSQC spectra with the necessary high spectral resolution along both ^{13}C and ^{1}H dimensions, nonuniform sampling in combination with pure shift spectroscopy was applied allowing the extraction of an abundance of unique cross-peaks belonging to hydrophobic compounds in complex lipidomics mixtures. As shown here, this information is critical for the unambiguous identification of underlying lipid molecules by means of the new COLMAR Lipids web server, also in combination with mass spectrometry, as is demonstrated for Caco-2 cell and lung tissue cell extracts.

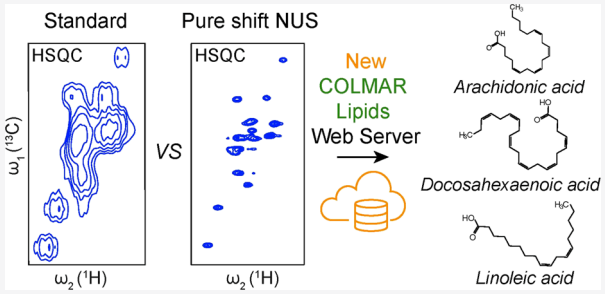

KEYWORDS: *lipids, NMR database, 2D HSQC, lipidomics, metabolomics*

INTRODUCTION

Lipids constitute structural components of the membranes of all living cells, provide energy storage and protection from physical and chemical influences, and play other critical functional roles, such as for cellular communication. Over the years, lipidomics has emerged as a subfield of systems biology aiming at the comprehensive understanding of the role of lipids in physiological processes,[1−3] including the metabolism and cellular functions of lipids in diseases, such as cancer, cardiovascular disorders, neurodegenerative diseases, obesity, and diabetes. Mass spectrometry combined with chromatography has become a popular platform for lipidomics studies to elucidate lipid composition in many different biological systems.[4] Nuclear magnetic resonance (NMR) spectroscopy has been used for the detailed structural characterization of lipid species.[5] One-dimensional (1D) proton nuclear magnetic resonance (^{1}H NMR) and ^{13}C NMR have proven useful for "coarse-grained" lipid profiling to characterize different classes of lipids in lipidomics mixtures.[6−10] For instance, the composition of unsaturated fatty acyl residues and allylic and divinyl carbons in rapeseed oil and soybean oil can be determined by ^{1}H and ^{13}C NMR spectra for quantitative analysis.[6] LipSpin has been introduced for the semiautomatic ^{1}H NMR spectra-based profiling of lipid extracts, providing quantitative information of major lipid classes in lipidomics mixtures, such as fatty acids, triglycerides, phospholipids, and cholesterols.[10] The composition and positions of acyl chains in the triacylglycerols of oil from *Moringa oleifera* were determined by ^{13}C NMR, demonstrating the detection of oleate, vaccenate, and eicosenoate chains.[7]

Multidimensional high-resolution solution NMR spectroscopy can provide detailed and unique fingerprint information of chemical compounds in complex chemical mixtures without the need for extensive sample purification/separation.[11−13] Two-dimensional (2D) ^{13}C-^{1}H heteronuclear single quantum

Received: December 11, 2019
Published: February 19, 2020

coherence (HSQC) has been applied for lipid profiling in a variety of lipid cell extracts.[14−16] Mycobacterial cell wall lipids were analyzed by 2D ^{13}C-^{1}H HSQC to monitor unique biomarker cross-peaks and test for the presence of certain lipid species to understand the role of lipids in mycobacteria pathogenesis.[14] 2D ^{13}C-^{1}H HSQC NMR was also used for phospholipid profiling of thermophilic *Geobacillus* sp. strain GWE1 isolated from sterilization ovens, which confirmed the ^{1}H and ^{13}C NMR assignments of the glycerol backbone position sn-1[17] and the $CH_2CH_2NH_2$ head group.[16] However, application of 2D HSQC to lipidomics mixtures for untargeted lipid identification and quantification is still very limited, which is partly due to the lack of curated and comprehensive lipid 2D NMR databases that are coupled with user-friendly platforms for spectral analysis. Moreover, certain lipids within the same lipid class share common substructures that tend to give rise to similar chemical shifts, requiring NMR spectra with very high resolution for their unambiguous discrimination (see Supporting Information, Figure S1).

Fortunately, nonuniform sampling (NUS) techniques enable the efficient acquisition of high-resolution 2D NMR spectra along the indirect dimension, thereby greatly benefitting metabolomics studies.[18,19] In addition, to boost the resolution along the direct proton dimension, broadband homonuclear decoupled "pure shift" methods have been adopted where peak multiplets collapse into singlets as the result of $^{1}H-^{1}H$ J coupling removal.[20,21] Importantly, the real-time pure shift (BIRD) HSQC improves not only spectral resolution but also affords a simultaneous gain in sensitivity.[22−26] Because the real-time pure shift technique works independently of the chosen NUS schedule along the indirect t_1 dimension, we combine it here with nonuniform sampling to simultaneously increase the resolution along both dimensions in 2D HSQC experiments of lipidomics samples.

We also introduce a new 2D HSQC hydrophobic compound database, which currently contains experimental 2D ^{13}C-^{1}H HSQC chemical shift data of 501 hydrophobic compounds, in tandem with a user-friendly NMR spectral analysis platform for lipid identification. This is implemented as a COLMAR Lipids web server, which is a new module of our public COLMAR suite of NMR web servers (http://spin.ccic.osu.edu/index.php/colmarm/index2). The high spectral resolution achieved in nonuniformly sampled 2D real-time pure shift HSQC spectra, which serve as input for COLMAR Lipids, enables the automated and unambiguous identification of lipid molecules in complex lipidomics mixtures. The approach is first tested for a lipid model mixture and then applied to hydrophobic extracts from Caco-2 human intestinal cells and mouse lung tissue.

METHODS AND EXPERIMENTAL SECTION

Hydrophobic Compound 2D ^{13}C-^{1}H HSQC Database

The hydrophobic 2D ^{13}C-^{1}H HSQC chemical shifts were retrieved from the existing HMDB, BMRB, and NMRShiftDB databases.[27−33] Only compounds with chemical shifts measured in 100% deuterated chloroform ($CDCl_3$) were used from these databases using either 4,4-dimethyl-4-silapentane-1-sulfonic acid (DSS) or tetramethylsilane (TMS) for chemical shift referencing. An in-house python script was developed to automatically read the source data document and obtain the compound name, CAS registry number (if applicable), chemical shifts (^{1}H and ^{13}C), smile strings, and molecular structures. This composite hydrophobic compound database contains lipids from a wide range of lipid classes, such as fatty acids, cholesterols, triglycerides, and phospholipids. It is currently the most comprehensive hydrophobic metabolite 2D ^{13}C-^{1}H HSQC database. For each compound, the chemical shifts were further subdivided into spin systems based on their molecular structure, allowing compound verification based on 2D TOCSY or 2D HSQC-TOCSY via our standard NMR metabolomics protocol implemented in the COLMARm web server.[34] Each database entry was manually inspected and compounds with incomplete data, such as a lack of ^{13}C chemical shifts, were removed. The hydrophobic compound data are stored in a relational database in a matrix form where each row belongs to a compound ID and each column denotes an attribute (e.g., ^{1}H chemical shift, CAS number). Currently, 501 hydrophobic compounds are stored in the COLMAR Lipids HSQC database, which is publicly accessible via the COLMAR Lipids web server (http://spin.ccic.osu.edu/index.php/colmarm/index2). Four hundred eighty-three of these compounds have at least one unique chemical shift whereas 17 compounds have all their chemical shifts overlapped with those of other database compounds.

Sample Preparation

Lipid mixture samples were prepared to test and apply the COLMAR Lipids web server on the NUS 2D real-time pure shift HSQC NMR spectra. A lipid model mixture was prepared containing four lipids: cholesterol (CAS: 57-88-5), linoleic acid (CAS: 60-33-3), arachidonic acid (CAS: 506-32-1), and docosahexaenoic acid (CAS: 6217-54-5). The final concentration of each compound was 2 mM in 600 μL of deuterated chloroform ($CDCl_3$) containing 0.03% (v/v) tetramethylsilane (TMS) for chemical shift referencing. The model mixture was transferred to a 5 mm NMR tube for NMR data collection.

Lung tissue was extracted from wild-type C57BL/6 mice and snap-frozen in liquid nitrogen. Lung samples (∼150 mg) were cut with a clean blade and added to a 1.5 mL Safe-Lock microcentrifuge tube (Eppendorf) with 600 μL of 1:1 methanol/double distilled H_2O (ddH_2O) and 300 μL of 1.4 mm stainless steel beads (SSB14B). The sample tube was inserted in a Bullet Blender (24 Gold BB24-AU by Next Advance) and homogenized at a speed of 10 for 12 min at 4 °C. Then, 400 μL of 1:1 methanol/ddH2O was added and the sample was centrifuged at 12,000 × *g* for 20 min at 4 °C to remove the beads and any remaining solid debris. The supernatant was collected and 3.5 mL of methanol, 3.5 mL of ddH_2O, and 4 mL of chloroform were added to a final methanol/ddH_2O/chloroform 1:1:1 (v/v/v) mixture. The sample was vortexed and centrifuged at 5000 × *g* for 20 min at 4 °C for separation of the aqueous and organic phases. The organic phase, which contains the lipids, was collected and dried using compressed nitrogen gas and stored at −80 °C until measurements were performed. The NMR sample was prepared by dissolving the dried sample in 600 μL of $CDCl_3$ with 0.03% (v/v) tetramethylsilane (TMS) for chemical shift referencing. The sample was then transferred to a 5 mm NMR tube with a Teflon cap and sealed with parafilm for NMR measurements.

Caco-2 cells are commonly used by pharmaceutical companies and for nutrition studies to understand nutrient absorption, as they mimic the small intestinal enterocyte (the primary site of gastrointestinal absorption) for both drugs and nutrients.[35−37] To date, only one NMR-based metabolomics study, which solely focused on polar analytes, that is, no lipids,

https://dx.doi.org/10.1021/acs.jproteome.9b00845
J. Proteome Res. 2020, 19, 1674−1683

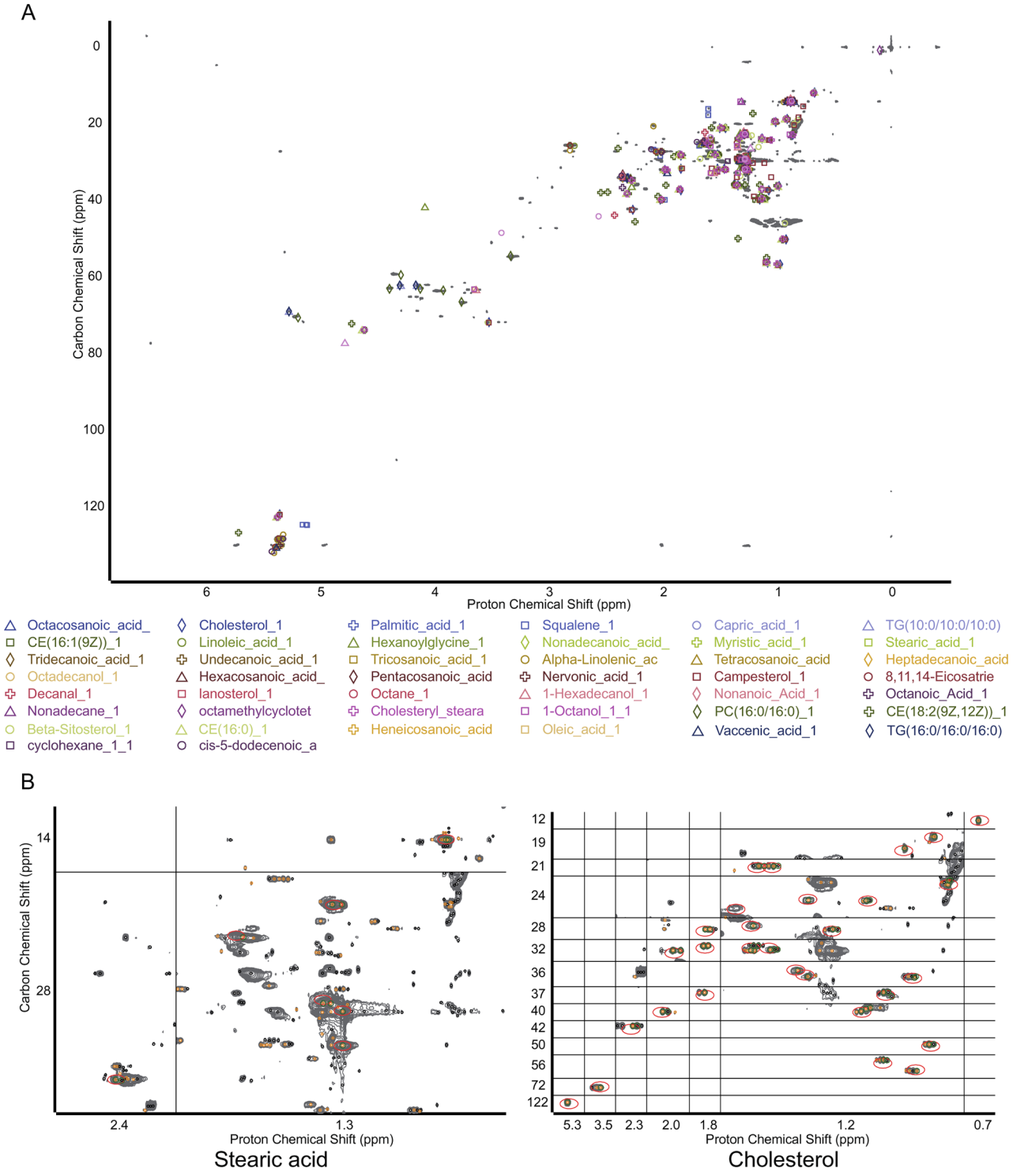

Figure 1. Untargeted identification of hydrophobic metabolites in Caco-2 cell extract with COLMAR Lipids web server. (A) Screenshot of annotated ^{13}C-^{1}H HSQC spectrum (above) with a list of hydrophobic metabolites identified by the web server (below). Each type of symbols belongs to the cross-peaks of a different hydrophobic metabolite in the COLMAR Lipids database. (B) Illustration of spectral matching of HSQC cross-peaks (red ellipses) by COLMAR Lipids web server of stearic acid (left) and cholesterol (right) allowing the identification of these metabolites in Caco-2 cell extract. The grid represents the automated concatenation of relevant spectral regions to facilitate visual inspection of matches.

has investigated their metabolome.[38] The Caco-2 cell model was utilized as previously described[39,40] with minor modifications as delineated below. Briefly, Caco-2 human intestinal cells (ATCC, #HTB-37, Rockville, MD) were grown as monolayers on 6-well plates and incubated at 37 °C under a modified atmosphere (i.e., 95% air, 5% CO_2) in a controlled humidity chamber (FormaSeriesII, Thermo Scientific). The media were changed every second day and consisted of DMEM with 15% fetal bovine serum (FBS) until confluence was reached, at which time FBS was reduced to 7.5% of the

https://dx.doi.org/10.1021/acs.jproteome.9b00845
J. Proteome Res. 2020, 19, 1674−1683

Table 1. Hydrophobic Metabolite Identification of Caco-2 Cell Extracts Using COLMAR Lipids Web Server[a,b]

metabolite name or ID	matching ratio[c]	^{13}C RMSD (ppm)	^{1}H RMSD (ppm)	uniqueness[d]	MS^{1} detected precursor ions[e]
octanoic acid	1.00	0.15	0.004	1	$[M + NH_4]^+$
tetracosanoic acid	1.00	0.12	0.009	1	$[M + NH_4]^+$
linoleic acid	1.00	0.13	0.012	1	$[M + NH_4]^+$
docosahexaenoic acid	0.95	0.08	0.008	4	$[M + H]^+$
eicosapentaenoic acid	0.94	0.10	0.008	1	$[M + H]^+$
1-hexadecanol	0.94	0.11	0.006	2	$[M + Na]^+$
PC (16:0/16:0)	0.71	0.12	0.006	4	$[M + Na]^+$
stigmasterol	0.65	0.10	0.010	5	$[M + H]^+$

[a]Abbreviations: TG = triglyceride, PC = phosphatidylcholine, CE = cholesterol ester [b]Identified lipids with uniqueness ≥1 and precursor ion(s) detected in UHPLC−HRMS. [c]The ratio of the matched number of peaks to the total number of peaks. [d]Number of cross-peaks in the HSQC spectrum of the mixture that are uniquely assigned to a certain metabolite. [e]Precursor ion species detected via UHPLC-Q-Tof with ESI positive, with $m/z \leq 5$ ppm of the predicted precursor mass.

medium. After cell differentiation (passage 27, 11−14 days postconfluence), cells were treated with artificial micelles diluted with fresh DMEM (1:4, v/v). Artificial micelles were prepared as previously described,[41] and their composition, including eicosapentaenoic acid (EPA) and docosahexaenoic acid (DHA), is listed in Table S1. Incubation occurred at 37 °C for 6 h, followed by several washes of 2 mL of PBS buffer + albumin and PBS buffer alone, and the monolayer was harvested using a cell scraper afterward. Cells were frozen at −80 °C for less than 4 weeks prior to analysis.

Lipids were extracted from cells using a modified Bligh−Dyer method, as described previously.[42] The extracts obtained from four wells were pooled to optimize the metabolite concentration for NMR analysis. Extracts were also analyzed using ultrahigh-performance liquid chromatography-high-resolution mass spectrometry (UHPLC−HRMS) using a 1290 UHPLC system interfaced with a Q-Tof 6545 (Agilent, Inc.) with an electrospray probe operated in a positive ion mode. A C18 column (Hypersil gold, 2.1 mm × 100 mm, 3 μm particle size) was employed using a water/acetonitrile gradient as previously described with the addition of 0.1% ammonium formate (w/v) as a solvent modifier.[43] The MS source settings were as follows: capillary voltage = +3000 V, nozzle voltage = 35 V, gas temperature = 300 ° C, drying gas flow = 10 L/min, nebulizer = 25 psi, sheath gas temperature = 350 ° C, and sheath gas flow = 12 L/min. The MS monitored m/z 50−1700 with an acquisition rate of 8119 transients per spectrum and 1 spectrum per second.

NMR Experiments and Processing

Uniformly (US) and nonuniformly sampled (NUS) 2D ^{13}C-^{1}H HSQC spectra were collected for the lipid model mixture and the lipid cell extracts with and without real-time broadband homonuclear BIRD decoupling pure shift methodology. All NMR spectra were acquired on a Bruker AVANCE III HD solution-state NMR spectrometer equipped with a cryogenically cooled TCI probe at 850 MHz proton frequency at 298 K. The standard US HSQC spectra and real-time pure shift US HSQC spectra of the lipid model mixture and lipid cell extracts were collected with 512 complex t_1 and 1024 complex t_2 points. The measurement time for each experiment was around 4 h. The spectral widths along the indirect and the direct dimensions were 34205.6 and 10204.1 Hz. The number of scans per t_1 increment was eight. The transmitter frequency offset values were 80 ppm in the ^{13}C dimension and 4.7 ppm in the ^{1}H dimension. For NUS NMR experiments, 12.5% NUS (i.e., 512 NUS complex points were selected out of 4096 uniformly sampled points in t_1) with and without real-time pure shift 2D HSQC spectra of the lipid model mixture, and lipid cell extracts were collected with a measurement time around 4 h. The number of scans per t_1 increment was eight. The transmitter frequency offset values were 80 ppm in the ^{13}C dimension and 4.7 ppm in the ^{1}H dimension. For the indirect carbon dimensions, the NUS spectra were processed with the IST algorithm implemented in the hmsIST software.[44] For all NUS spectra, the t_1 increments were selected using a Poisson-gap distribution using the hmsIST software's schedule generator with default parameters (sinusoidal weight is 2 with random seed generator).[45] Both the NUS and US NMR data were zero-filled, Fourier-transformed, and phase-corrected with final digital resolution 4096 (ω_2) × 8192 (ω_1) (real) points using the Bruker Topspin 3.5 software. Chemical shift database query and identification of metabolites from the 2D NMR spectra were performed using the COLMAR NMR webserver (http://spin.ccic.ohio-state.edu/index.php/colmar). The study has been registered with MetaboLights with identifier MTBLS1470 (www.ebi.ac.uk/metabolights/MTBLS1470).

RESULTS AND DISCUSSION

COLMAR Lipids Web Server with Hydrophobic Metabolite 2D HSQC Database

The COLMAR Lipids web server was implemented as a new module in the COLMAR suite of NMR web servers, designed for the automated analysis of 2D ^{13}C-^{1}H HSQC spectra of lipidomics mixtures. Because all spectra need to be properly referenced before being queried against the lipid database, the COLMAR Lipids web server allows users to reference the chemical shifts based on an internal standard, such as tetramethylsilane (TMS) or a lipid with known chemical shifts present in the sample. After referencing the HSQC spectrum, the query algorithm embedded in the COLMAR web server performs automated matching with database compounds. The default values for the error tolerance for ^{1}H and ^{13}C chemical shifts are 0.03 and 0.3 ppm, respectively, and can be changed by the user. Figure 1 is a screenshot of lipid compound identification in Caco-2 cell extract by the new COLMAR Lipids web server together with examples of matched peaks and spectral regions of identified compounds. It demonstrates the high spectral resolution achievable for lipidomics samples necessary for the accurate identification of lipid metabolites. Table 1 provides the lipids (uniqueness >0 and precursor ion(s) (MS1) detected in UHPLC−HRMS) identified in Caco-2 cell extract. Displayed are quantitative metrics based on a standard 2D ^{13}C-^{1}H HSQC spectrum including matching

https://dx.doi.org/10.1021/acs.jproteome.9b00845
J. Proteome Res. 2020, 19, 1674−1683

ratios (number of cross-peaks identified of a given metabolite divided by the number of cross-peaks expected for this compound), chemical shift RMSDs (for both ^{13}C and ^{1}H), uniqueness (number of cross-peaks uniquely assigned to a given compound), and the detected precursor ion(s) (MS1) of the lipid. The "uniqueness" metric reflects the number of unique peaks of a compound present in the spectrum, which allows one to determine whether at least one cross-peak of an identified compound does not overlap with peaks of other database compounds. The complete lipid identification results in Caco-2 cell extract and lung tissue are provided in Tables S3 and S4. As can be seen in the lipid identification in Tables S3 and S4 of Caco-2 cell extract and lung tissue, a number of lipids exist with uniqueness ≥ 1, which means that one or more distinct peaks of these lipids were found, which uniquely belong to them (i.e., there are no other cross-peaks within a distance of 0.03 ppm (^{1}H) or 0.3 ppm (^{13}C)). Such peaks have the potential to serve as diagnostic biomarker(s) by confirming the presence or absence of a particular lipid molecule and allow one to elucidate the cellular origins of a particular lipid.

An additional benefit of the hydrophobic metabolite 2D HSQC NMR database is that it allows identification of structural isomers that may not be easily distinguished by mass spectrometry (MS or MS/MS) alone (Figure S2). For example, isomers decanal and menthol generate highly similar MS/MS spectra, whereas the 2D HSQC spectra of decanal and menthol show very different nonoverlapping cross-peaks, which makes a distinction between these isomers straightforward.

The COLMAR Lipids webserver works mostly automatically, including peak picking, spectral referencing, and database query, after the input spectra have been uploaded and parameters for peak-picking, spectral referencing, matching ratio, and ^{1}H and ^{13}C chemical shift RMSD ratio cutoffs have been accepted or modified.

Disambiguation of Lipid Identification Using Complementary Information

COLMAR Lipids generates a list of hydrophobic compound candidates based on a single 2D HSQC spectrum. However, due to the high similarity of certain lipids and of their chemical shifts, some HSQC peaks are assigned to multiple compounds simultaneously, which can lower the uniqueness scores all the way to zero (Tables S3 and S4), thereby reducing the confidence in the accuracy of these compounds. For instance, COLMAR Lipids returns TG(16:0/16:0/16:0) and TG(10:0/10:0/10:0) with high matching ratios of 1.0 (10 out of 10 database peaks are matched) and 0.91 (10/11 database peaks are matched), respectively, whereas the uniqueness scores of both compounds are zero. The two compounds have very similar chemical shifts and share four cross-peaks. Hence, complementary experimental information, such as mass information, is needed to cross-validate and disambiguate the identified compounds. By combining COLMAR Lipids results of the Caco-2 cell extract with liquid chromatography−mass spectrometry (LC−MS) data, a number of lipids could be confirmed and others were excluded, thereby reducing the false positive rate (Table S3).

Additional opportunities exist in leveraging the COLMAR approach, in combination with empirically derived LC−MS and LC−MS/MS spectra obtained from the same samples, to conclusively identify more challenging lipids. Certainly, MS/MS confers some advantages in lipid identification, for example, fatty acyl positional isomers of di- and tri-glycerides can be established by studying fragmentation patterns, with fatty acid loss in the outer position (sn-1 or sn-3) favored over the sn-2 position.[46] However, accurate annotation of geometric (i.e., cis-trans) isomers by LC−MS has not been possible in the absence of authentic standards until recently. Ion mobility spectrometry (IMS) is making notable progress in this area.[47,48] However, low ion transmission through the ion mobility drift tube reduces sensitivity and in the past has limited applicability to biological samples with finite concentrations of metabolites,[49,50] although recent improvements, incorporating ion focusing guides and utilizing electrodynamic or electrostatic focusing fields, have improved transmission efficiency.[50] Likewise, accurate identification of unsaturated double bond positions remains cumbersome by LC−MS, requiring an online ozone source[51] or in-line acetone photo-derivatization via the Paternó−Büchi reaction.[52] In contrast, utilizing COLMAR in combination with LC-fractionation, exact mass, and fragmentation data will open up alternative strategies for the accurate annotation of such common types of complex lipid mixtures.

Accurate Lipid Identification by High-Resolution 2D NUS Real-Time Pure Shift HSQC

For some lipids and fatty acids, for example, linoleic acid (LA) and arachidonic acid (AA), which share common substructures, their chemical shifts can be very similar as a result cross-peaks from common substructures tend to overlap in a standard HSQC spectrum, for example, one with digital resolution of 4096 (ω_2) × 1024 (ω_1) real data points. By contrast, resolution enhancement along the indirect ^{13}C dimension by NUS and along the direct ^{1}H dimension by pure shift NMR resolves many of the overlaps without increasing the measurement time over the standard HSQC experiment. This permits the unique identification of hydrophobic compounds as it is demonstrated for both a model mixture and two real-world lipid mixtures. Figure 2 shows a spectral comparison between US and NUS 2D HSQC spectra with and without the real-time pure shift technique for the lipid model mixture. The US HSQC spectra were acquired with 512 complex points along the indirect ^{13}C dimension. The NUS HSQC spectra were acquired with 512 NUS points out of 4096 complex points (12.5% sampling) along the indirect ^{13}C dimension. Hence, the NUS increments were selected from an 8 times larger indirect evolution time t_1 range than the US spectrum resulting in ultrahigh resolution along ω_1. All spectra were processed or reconstructed to a final digital resolution of 4096 (ω_2) × 8192 (ω_1) real data points. In the alkene carbon region, where structurally similar fatty acids tend to generate similar chemical shifts, the NUS spectra not only provide substantially higher resolution than the US spectra allowing the easier identification of individual cross-peaks with more precise peak positions but also show a larger number of distinct peaks than the US spectra. In particular, the cross-peaks in the NUS HSQC spectrum of arachidonic acid, docosahexaenoic acid, and linoleic acid are clearly separated (Figure 2). As indicated by the black square box in Figure 2e, arachidonic acid, docosahexaenoic acid, and linoleic acid have a similar proton and carbon chemical shift distribution (^{1}H: 5.38−5.41 ppm, ^{13}C: 127.8−128.2 ppm). For example, the ^{13}C chemical shift difference of the two closest peaks from arachidonic acid and linoleic acid is only 0.0966 ppm (i.e., 20.65 Hz on an 850 MHz NMR spectrometer). To achieve a

https://dx.doi.org/10.1021/acs.jproteome.9b00845
J. Proteome Res. 2020, 19, 1674−1683

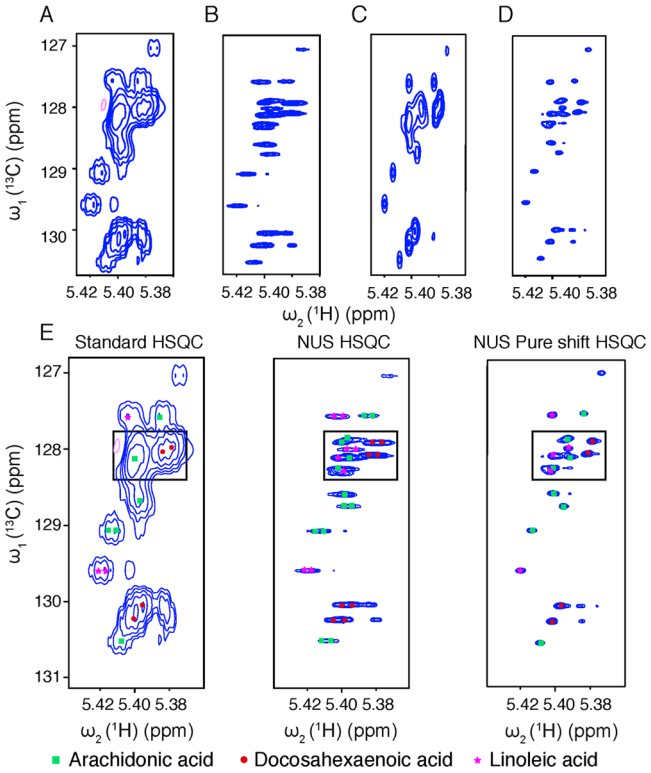

Figure 2. Comparison of performance of different 2D ^{13}C-^{1}H HSQC experiments in the CH═CH region for lipid identification in a model mixture. (A) Uniformly sampled standard HSQC (2048 (t_2) × 512 (t_1) complex points). (B) Nonuniformly sampled (NUS) HSQC (12.5% NUS and 512 NUS points, 2048 (t_2) × 4096 (t_1) complex points). (C) Uniformly sampled real-time pure shift HSQC (2048 (t_2) × 512 (t_1) complex points). (D) Nonuniformly sampled real-time pure shift HSQC (12.5% NUS and 512 NUS points, 2048 (t_2) × 4096 (t_1) complex points). (E) Lipid identification in standard 2D HSQC, 2D NUS HSQC, and 2D NUS pure shift HSQC spectra of the model mixture. All spectra were processed to final spectral digital resolution of 4096 (ω_2) × 8192 (ω_1) points.

digital resolution that distinguishes these two peaks in a traditional US HSQC spectrum, according to the Nyquist sampling theorem, at least 1502 complex points along t_1 are needed (with carbon spectral width of 145 ppm). Traditional data processing techniques, such as zero-filling and linear prediction, have a very limited effect on the improvement of the digital resolution, as is shown in Figure 2c. To boost the resolution to that of a US HSQC with 4096 complex t_1 points at the same measurement time as a US HSQC with 512 complex t_1 points, NUS can be employed and combined with real-time pure shift techniques along t_2 (Figure 2b,d). The latter provides broadband homonuclear proton−proton decoupling, which causes the multiplet signals to collapse into singlets along the ^{1}H dimension, which further separate cross-peaks, simplify the spectra, and enhance sensitivity as well. On the other hand, the relatively long ^{13}C T_2 relaxation times cause some minor sensitivity loss by NUS where the longest t_1 increment is up to 8 times longer than in the standard HSQC.

The spectral resolution benefits for lipid metabolism studies are demonstrated by applying the high-resolution NUS pure shift NMR strategy to Caco-2 cell extracts to study their cellular uptake of eicosapentaenoic acid (EPA) and docosahexaenoic acid (DHA). Both EPA and DHA are long-chain omega-3 fatty acids found primarily in the human diet in cold-water fish oil.[53] EPA and DHA serve as key precursors to important metabolites that play roles in inflammatory signaling,[54] as well as visual and neural development.[55] Caco-2 cells were incubated with artificial micelle formulations with varying ratios of EPA, DHA, and OA (Table S1). Due to the high structural similarity (Tanimoto similarity coefficient of 0.704), the chemical shifts tend to be very similar necessitating ultrahigh-resolution NMR to distinguish between the two molecules. 2D HSQC and 2D NUS HSQC with and without pure shift methodology were applied. In Figure 3, the

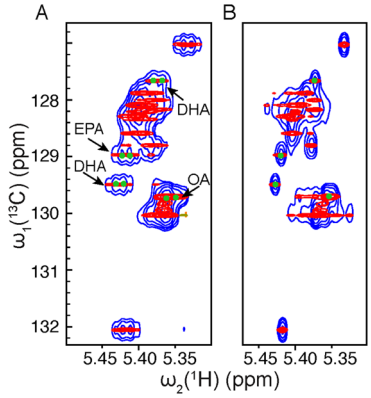

Figure 3. Identification of eicosapentaenoic acid (EPA) and docosahexaenoic acid (DHA) in different variants of 2D ^{13}C-^{1}H HSQC experiments of Caco-2 cell extract. (A) Identification of EPA and DHA in a uniformly sampled standard HSQC (blue, 2048 (t_2) × 512 (t_1) complex points) and a nonuniformly sampled standard HSQC (red, 12.5% NUS and 512 NUS points, 2048 (t_2) × 4096 (t_1) complex points). (B) Identification of EPA and DHA in a uniformly sampled real-time pure shift HSQC (blue, 2048 (t_2) × 512 (t_1) complex points) and the nonuniformly sampled real-time pure shift HSQC (red, 12.5% NUS and 512 NUS points, 2048 (t_2) × 4096 (t_1) complex points). All spectra were processed to a final spectral digital resolution of 4096 (ω_2) × 8192 (ω_1). Unique cross-peaks that belong to docosahexaenoic acid (DHA), eicosapentaenoic acid (EPA), and oleic acid (OA) are labeled by green dots.

unambiguous identification of EPA and DHA in the complex Caco-2 cell extract is demonstrated by using NUS HSQC spectra with and without the real-time pure shift technique. Specifically, the alkene carbon CH═CH peaks in DHA and EPA are clearly separated in the 2D NUS HSQC, while they severely overlap in the normal 2D HSQC. The uniquely identified cross-peaks of the CH═CH groups help identify and quantify EPA and DHA in this complex mixture. Caco-2 cells were incubated with micelles containing six different formulations of EPA, DHA, and OA (Table S2). These can be clearly differentiated and identified by the high-resolution NUS 2D standard HSQC spectra (Figure 4) but are barely distinguishable by the 1D ^{1}H NMR or standard 2D HSQC spectra. Furthermore, this information can be utilized to quantitate the cellular uptake of EPA, DHA, and OA from the micelles, as will be reported elsewhere.

A significant improvement of resolution in the NUS HSQC experiment can also be seen in other crowded regions. Figure S3 shows a comparison between the uniformly sampled HSQC and NUS HSQC of Caco-2 cell extract and lung tissue by acquiring 512 complex points along the indirect ^{13}C dimension. All spectra were processed or reconstructed to a final digital resolution of 4096 (ω_2) × 8192 (ω_1) real data

https://dx.doi.org/10.1021/acs.jproteome.9b00845
J. Proteome Res. 2020, 19, 1674−1683

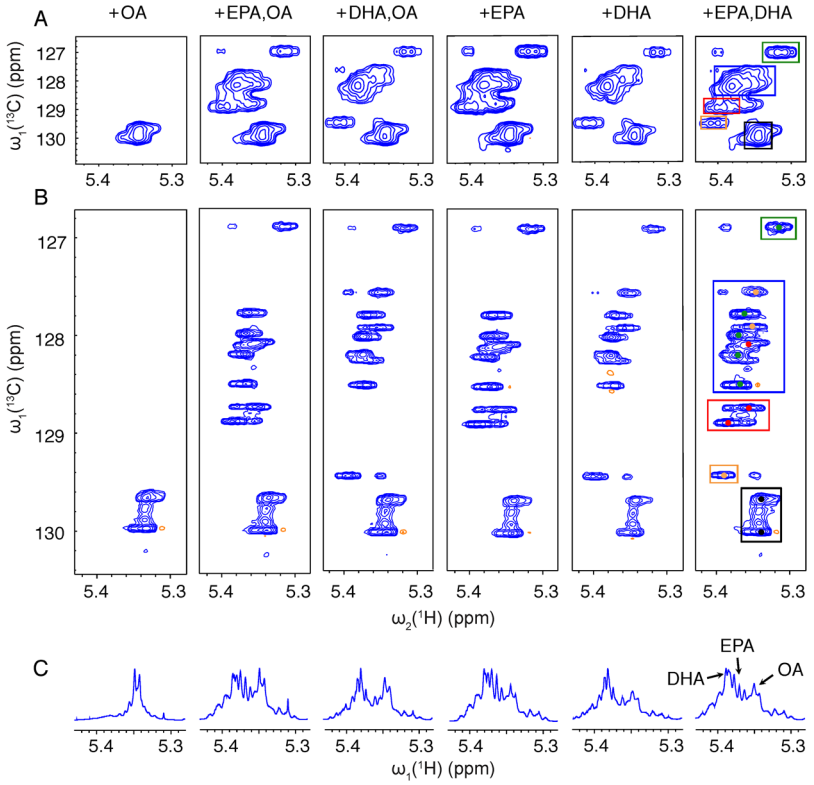

Figure 4. Differentiation of Caco-2 cells by NMR metabolomics analysis. NMR spectra of Caco-2 cells incubated with micelles containing different concentrations of docosahexaenoic acid (DHA), eicosapentaenoic acid (EPA), and oleic acid (OA) are provided in each column (the details of each micelle formulation are provided in Table S2). "(A) Alkene carbon region of standard uniformly sampled HSQC spectra (2048 (t_2) × 512 (t_1) complex points). (B) Alkene carbon region of standard nonuniformly sampled HSQC spectra (12.5% NUS and 512 NUS points, 2048 (t_2) × 4096 (t_1) complex points). (C) Alkene carbon region of the 1D ^{1}H NMR spectra. In the rightmost column, DHA, EPA, and OA peaks are annotated as follows: the green box contains overlapping peaks of DHA and EPA (green dots), the red box contains cross-peaks of EPA only (red dots), the yellow box of DHA only (yellow dots), the black box contains peaks that belong to OA only (black dots), and the blue box contains peaks of DHA and EPA.

points. The resolution along the carbon dimension in the NUS HSQC is much higher than that in the standard HSQC spectrum with a digital resolution of 7.58 Hz (NUS) versus 60.66 Hz (US) acquired on an 850 MHz NMR spectrometer. As a direct consequence, the NUS HSQC spectra produce numerous well-isolated peaks in crowded regions, especially when combined with pure shift methodology along the proton dimension, as indicated in Figure S3B,D,F,H.

It should be noted that the majority of hydrophobic compounds in the COLMAR Lipids database contain (^{1}H, ^{13}C) chemical shift information that was measured using regular HSQCs with 512 complex points along the indirect ^{13}C dimension. As shown in Figure 3, structurally similar lipid compounds such as EPA and DHA share 13 out of 18 cross-peaks at virtually identical positions in the low-resolution HSQC spectrum, which illustrates the challenge of lipidomics by traditional 2D NMR. Therefore, for lipid identification and analysis by high-resolution NUS real-time pure shift HSQC, we recommend that future reference lipid target compounds are measured using these types of high-resolution HSQC experiments.

In addition, even an extremely low sparseness rate of the NUS sampling schedule (e.g., as low as 6.25%, 256 NUS complex points along t_1) hardly affects spectral reconstruction quality. Figure S4 shows a comparison of an NUS HSQC NMR spectrum of lung tissue with 6.25% sparseness with the corresponding US NMR spectrum with the same number of t_1 increments. The reconstructed NUS HSQC and US HSQC spectra display almost the same peak profile. For this real-world lipidomics mixture, this demonstrates both the feasibility and clear benefits of up to 16-fold improved spectral resolution along the indirect dimension without a concomitant increase of measurement time.

■ CONCLUSIONS

The integration of the new 2D ^{13}C-^{1}H HSQC lipid database into COLMAR enables the unique identification of many lipids present in complex lipidomics mixtures. To maximize the number of identified compounds and minimize false positives, the highest possible NMR spectral resolution is crucial. As demonstrated here, it can be achieved by performing the NMR experiments at high magnetic fields in combination with the use of nonuniformly sampled (NUS) pure shift methodology to simultaneously optimize the resolution along both the ^{13}C and ^{1}H dimensions. Highly crowded HSQC regions, such as the alkene region, can thereby be resolved into individual cross-peaks, which dramatically improves the identification accuracy of lipids in complex lipidomics mixtures. We anticipate that the new relational 2D ^{13}C-^{1}H HSQC hydrophobic compound database that can be queried via the COLMAR web server will significantly facilitate and promote the application of 2D NMR-based lipidomics, and its combination with MS, for a variety of hydrophobic biological mixtures.

https://dx.doi.org/10.1021/acs.jproteome.9b00845
J. Proteome Res. 2020, 19, 1674−1683

■ ASSOCIATED CONTENT

Supporting Information

The Supporting Information is available free of charge at https://pubs.acs.org/doi/10.1021/acs.jproteome.9b00845.

Figure S1, 1D ^{1}H and 2D ^{13}C-^{1}H HSQC NMR spectra of Caco-2 cell extract; Figure S2, comparison of 2D ^{13}C-^{1}H HSQC NMR spectra and LC−MS/MS spectra pairs of structural isomers; Figure S3, spectral comparison of crowded regions of different types of 2D ^{13}C-^{1}H HSQC experiments in Caco-2 cell extract and lung tissue; Figure S4, spectral comparison of 6.25% NUS HSQC NMR spectrum (red) and US HSQC spectrum (blue) of mouse lung tissue extracts; Table S1, composition of artificial micelles incubated with Caco-2 human intestinal cells for 6 h prior to experiment termination; Table S2, different ratios of fatty acids utilized in the micelles with which Caco-2 human intestinal cells were incubated for 6 h; Table S3, hydrophobic metabolite identification results of lung tissue by COLMAR Lipids web serve; and Table S4, different amounts of fatty acids used for growing Caco-2 human intestinal cells (PDF)

■ AUTHOR INFORMATION

Corresponding Author

Rafael Brüschweiler − *Department of Chemistry and Biochemistry, Campus Chemical Instrument Center, and Department of Biological Chemistry and Pharmacology, The Ohio State University, Columbus, Ohio 43210, United States*; Email: bruschweiler.1@osu.edu

Authors

Cheng Wang − *Department of Chemistry and Biochemistry, The Ohio State University, Columbus, Ohio 43210, United States*

István Timári − *Department of Chemistry and Biochemistry, The Ohio State University, Columbus, Ohio 43210, United States*

Bo Zhang − *Department of Chemistry and Biochemistry, The Ohio State University, Columbus, Ohio 43210, United States*

Da-Wei Li − *Campus Chemical Instrument Center, The Ohio State University, Columbus, Ohio 43210, United States*; orcid.org/0000-0002-3266-5272

Abigail Leggett − *Ohio State Biochemistry Program, The Ohio State University, Columbus, Ohio 43210, United States*

Amal O. Amer − *Department of Microbiology, The Ohio State University, Columbus, Ohio 43210, United States*

Lei Bruschweiler-Li − *Campus Chemical Instrument Center, The Ohio State University, Columbus, Ohio 43210, United States*

Rachel E. Kopec − *Department of Human Sciences and Foods for Health Discovery Theme, The Ohio State University, Columbus, Ohio 43210, United States*; orcid.org/0000-0002-1368-6713

Complete contact information is available at: https://pubs.acs.org/10.1021/acs.jproteome.9b00845

Notes

The authors declare no competing financial interest.

■ ACKNOWLEDGMENTS

This work was supported by graduate fellowships from Foods for Health (to C.W. and B.Z.), a focus area of the Discovery Themes Initiative at OSU, a postdoctoral fellowship from the former President of Hungary, Dr. László Sólyom (to I. T.), and the National Institutes of Health (grant R01 GM066041 (to R.B.)). We thank Drs. Chureeporn Chitchumroonchokchai and Mark Failla for valuable advice regarding the Caco-2 cell experiments. All NMR experiments were performed at the Campus Chemical Instrument Center NMR facility at the Ohio State University.

■ REFERENCES

(1) Wenk, M. R. The emerging field of lipidomics. *Nat. Rev. Drug Discovery* **2005**, *4*, 594−610.

(2) Dennis, E. A. Lipidomics joins the omics evolution. *Proc. Natl. Acad. Sci. U. S. A.* **2009**, *106*, 2089−2090.

(3) Wenk, M. R. Lipidomics: new tools and applications. *Cell* **2010**, *143*, 888−895.

(4) Cajka, T.; Fiehn, O. Toward Merging Untargeted and Targeted Methods in Mass Spectrometry-Based Metabolomics and Lipidomics. *Anal. Chem.* **2016**, *88*, 524−545.

(5) Li, J.; Vosegaard, T.; Guo, Z. Applications of nuclear magnetic resonance in lipid analyses: An emerging powerful tool for lipidomics studies. *Prog. Lipid Res.* **2017**, *68*, 37−56.

(6) Miyake, Y.; Yokomizo, K.; Matsuzaki, N. Determination of unsaturated fatty acid composition by high-resolution nuclear magnetic resonance spectroscopy. *J. Am. Oil Chem. Soc.* **1998**, *75*, 1091−1094.

(7) Vlahov, G.; Chepkwony, P. K.; Ndalut, P. K. 13C NMR Characterization of Triacylglycerols of Moringa oleifera Seed Oil: An "Oleic-Vaccenic Acid" Oil. *J. Agric. Food Chem.* **2002**, *50*, 970−975.

(8) Tugnoli, V.; Bottura, G.; Fini, G.; Reggiani, A.; Tinti, A.; Trinchero, A.; Tosi, M. R. 1H-NMR and 13C-NMR lipid profiles of human renal tissues. *Biopolymers* **2003**, *72*, 86−95.

(9) Barison, A.; da Silva, C. W.; Campos, F. R.; Simonelli, F.; Lenz, C. A.; Ferreira, A. G. A simple methodology for the determination of fatty acid composition in edible oils through 1H NMR spectroscopy. *Magn. Reson. Chem.* **2010**, *48*, 642−650.

(10) Barrilero, R.; Gil, M.; Amigó, N.; Dias, C. B.; Wood, L. G.; Garg, M. L.; Ribalta, J.; Heras, M.; Vinaixa, M.; Correig, X. LipSpin: A New Bioinformatics Tool for Quantitative (1)H NMR Lipid Profiling. *Anal. Chem.* **2018**, *90*, 2031−2040.

(11) Bingol, K.; Brüschweiler, R. Multidimensional approaches to NMR-based metabolomics. *Anal. Chem.* **2013**, *86*, 47−57.

(12) Marchand, J.; Martineau, E.; Guitton, Y.; Dervilly-Pinel, G.; Giraudeau, P. Multidimensional NMR approaches towards highly resolved, sensitive and high-throughput quantitative metabolomics. *Curr. Opin. Biotechnol.* **2017**, *43*, 49−55.

(13) Alexandri, E.; Ahmed, R.; Siddiqui, H.; Choudhary, M. I.; Tsiafoulis, C. G.; Gerothanassis, I. P. High Resolution NMR Spectroscopy as a Structural and Analytical Tool for Unsaturated Lipids in Solution. *Molecules* **2017**, *22*, 1663.

(14) Mahrous, E. A.; Lee, R. B.; Lee, R. E. A rapid approach to lipid profiling of mycobacteria using 2D HSQC NMR maps. *J. Lipid Res.* **2008**, *49*, 455−463.

(15) Hatzakis, E.; Agiomyrgianaki, A.; Kostidis, S.; Dais, P. High-Resolution NMR Spectroscopy: An Alternative Fast Tool for Qualitative and Quantitative Analysis of Diacylglycerol (DAG) Oil. *J. Am. Oil Chem. Soc.* **2011**, *88*, 1695−1708.

(16) Shah, S. P.; Jansen, S. A.; Taylor, L. J.-A.; Chong, P. L.-G.; Correa-Llantén, D. N.; Blamey, J. M. Lipid composition of thermophilic Geobacillus sp. strain GWE1, isolated from sterilization oven. *Chem. Phys. Lipids* **2014**, *180*, 61−71.

(17) Bittman, R. Glycerolipids: Chemistry. In *Encyclopedia of Biophysics*; Roberts, G. C. K., Ed.; Springer Berlin Heidelberg: Berlin, Heidelberg, 2013; pp 907−914.

(18) Le Guennec, A.; Dumez, J. N.; Giraudeau, P.; Caldarelli, S. Resolution-enhanced 2D NMR of complex mixtures by non-uniform sampling. *Magn. Reson. Chem.* **2015**, *53*, 913−920.
(19) Li, D.; Hansen, A. L.; Bruschweiler-Li, L.; Brüschweiler, R. Non-Uniform and Absolute Minimal Sampling for High-Throughput Multidimensional NMR Applications. *Chem. − Eur. J.* **2018**, *24*, 11535−11544.
(20) Castañar, L.; Parella, T. Broadband 1H homodecoupled NMR experiments: recent developments, methods and applications. *Magn. Reson. Chem.* **2015**, *53*, 399−426.
(21) Zangger, K. Pure shift NMR. *Prog. Nucl. Magn. Reson. Spectrosc.* **2015**, *86-87*, 1−20.
(22) Paudel, L.; Adams, R. W.; Király, P.; Aguilar, J. A.; Foroozandeh, M.; Cliff, M. J.; Nilsson, M.; Sándor, P.; Waltho, J. P.; Morris, G. A. Simultaneously enhancing spectral resolution and sensitivity in heteronuclear correlation NMR spectroscopy. *Angew. Chem., Int. Ed. Engl.* **2013**, *52*, 11616−11619.
(23) Pérez-Trujillo, M.; Castañar, L.; Monteagudo, E.; Kuhn, L. T.; Nolis, P.; Virgili, A.; Williamson, R. T.; Parella, T. Simultaneous (1)H and (13)C NMR enantiodifferentiation from highly-resolved pure shift HSQC spectra. *Chem. Commun.* **2014**, *50*, 10214−10217.
(24) Farjon, J.; Milande, C.; Martineau, E.; Akoka, S.; Giraudeau, P. The FAQUIRE Approach: FAst, QUantitative, hIghly Resolved and sEnsitivity Enhanced (1)H, (13)C Data. *Anal. Chem.* **2018**, *90*, 1845−1851.
(25) Kiraly, P.; Nilsson, M.; Morris, G. A. Practical aspects of real-time pure shift HSQC experiments. *Magn. Reson. Chem.* **2018**, *56*, 993−1005.
(26) Timári, I.; Wang, C.; Hansen, A. L.; Costa Dos Santos, G.; Yoon, S. O.; Bruschweiler-Li, L.; Brüschweiler, R. Real-Time Pure Shift HSQC NMR for Untargeted Metabolomics. *Anal. Chem.* **2019**, *91*, 2304−2311.
(27) Steinbeck, C.; Krause, S.; Kuhn, S. NMRShiftDB-constructing a free chemical information system with open-source components. *J. Chem. Inf. Comput. Sci.* **2003**, *43*, 1733−1739.
(28) Steinbeck, C.; Kuhn, S. NMRShiftDB – compound identification and structure elucidation support through a free community-built web database. *Phytochemistry* **2004**, *65*, 2711−2717.
(29) Wishart, D. S.; Tzur, D.; Knox, C.; Eisner, R.; Guo, A. C.; Young, N.; Cheng, D.; Jewell, K.; Arndt, D.; Sawhney, S.; Fung, C.; Nikolai, L.; Lewis, M.; Coutouly, M. A.; Forsythe, I.; Tang, P.; Shrivastava, S.; Jeroncic, K.; Stothard, P.; Amegbey, G.; Block, D.; Hau, D. D.; Wagner, J.; Miniaci, J.; Clements, M.; Gebremedhin, M.; Guo, N.; Zhang, Y.; Duggan, G. E.; Macinnis, G. D.; Weljie, A. M.; Dowlatabadi, R.; Bamforth, F.; Clive, D.; Greiner, R.; Li, L.; Marrie, T.; Sykes, B. D.; Vogel, H. J.; Querengesser, L. HMDB: the Human Metabolome Database. *Nucleic Acids Res.* **2007**, *35*, D521−D526.
(30) Ulrich, E. L.; Akutsu, H.; Doreleijers, J. F.; Harano, Y.; Ioannidis, Y. E.; Lin, J.; Livny, M.; Mading, S.; Maziuk, D.; Miller, Z.; Nakatani, E.; Schulte, C. F.; Tolmie, D. E.; Wenger, R. K.; Yao, H.; Markley, J. L. BioMagResBank. *Nucleic Acids Res.* **2007**, *36*, D402−D408.
(31) Wishart, D. S.; Jewison, T.; Guo, A. C.; Wilson, M.; Knox, C.; Liu, Y.; Djoumbou, Y.; Mandal, R.; Aziat, F.; Dong, E.; Bouatra, S.; Sinelnikov, I.; Arndt, D.; Xia, J.; Liu, P.; Yallou, F.; Bjorndahl, T.; Perez-Pineiro, R.; Eisner, R.; Allen, F.; Neveu, V.; Greiner, R.; Scalbert, A. HMDB 3.0–The Human Metabolome Database in 2013. *Nucleic Acids Res.* **2012**, *41*, D801−D807.
(32) Kuhn, S.; Schlörer, N. E. Facilitating quality control for spectra assignments of small organic molecules: nmrshiftdb2–a free in-house NMR database with integrated LIMS for academic service laboratories. *Magn. Reson. Chem.* **2015**, *53*, 582−589.
(33) Wishart, D. S.; Feunang, Y. D.; Marcu, A.; Guo, A. C.; Liang, K.; Vázquez-Fresno, R.; Sajed, T.; Johnson, D.; Li, C.; Karu, N.; Sayeeda, Z.; Lo, E.; Assempour, N.; Berjanskii, M.; Singhal, S.; Arndt, D.; Liang, Y.; Badran, H.; Grant, J.; Serra-Cayuela, A.; Liu, Y.; Mandal, R.; Neveu, V.; Pon, A.; Knox, C.; Wilson, M.; Manach, C.; Scalbert, A. HMDB 4.0: the human metabolome database for 2018. *Nucleic Acids Res.* **2018**, *46*, D608−D617.
(34) Bingol, K.; Li, D.-W.; Zhang, B.; Brüschweiler, R. Comprehensive Metabolite Identification Strategy Using Multiple Two-Dimensional NMR Spectra of a Complex Mixture Implemented in the COLMARm Web Server. *Anal. Chem.* **2016**, *88*, 12411−12418.
(35) Hidalgo, I. J.; Raub, T. J.; Borchardt, R. T. Characterization of the human colon carcinoma cell line (Caco-2) as a model system for intestinal epithelial permeability. *Gastroenterology* **1989**, *96*, 736−749.
(36) Delie, F.; Rubas, W. A human colonic cell line sharing similarities with enterocytes as a model to examine oral absorption: advantages and limitations of the Caco-2 model. *Crit. Rev. Ther. Drug Carrier Syst.* **1997**, *14*, 221−286.
(37) Englund, G.; Rorsman, F.; Rönnblom, A.; Karlbom, U.; Lazorova, L.; Gråsjö, J.; Kindmark, A.; Artursson, P. Regional levels of drug transporters along the human intestinal tract: co-expression of ABC and SLC transporters and comparison with Caco-2 cells. *Eur. J. Pharm. Sci.* **2006**, *29*, 269−277.
(38) Lee, I. J.; Hom, K.; Bai, G.; Shapiro, M. NMR metabolomic analysis of caco-2 cell differentiation. *J. Proteome Res.* **2009**, *8*, 4104−4108.
(39) Garrett, D. A.; Failla, M. L.; Sarama, R. J. Development of an in vitro digestion method to assess carotenoid bioavailability from meals. *J. Agric. Food Chem.* **1999**, *47*, 4301−4309.
(40) Zhong, S.; Vendrell-Pacheco, M.; Heskitt, B.; Chitchumroonchokchai, C.; Failla, M.; Sastry, S. K.; Francis, D. M.; Martin-Belloso, O.; Elez-Martínez, P.; Kopec, R. E. Novel Processing Technologies as Compared to Thermal Treatment on the Bioaccessibility and Caco-2 Cell Uptake of Carotenoids from Tomato and Kale-Based Juices. *J. Agric. Food Chem.* **2019**, *67*, 10185−10194.
(41) Chitchumroonchokchai, C.; Schwartz, S. J.; Failla, M. L. Assessment of lutein bioavailability from meals and a supplement using simulated digestion and caco-2 human intestinal cells. *J. Nutr.* **2004**, *134*, 2280−2286.
(42) Kopec, R. E.; Caris-Veyrat, C.; Nowicki, M.; Bernard, J. P.; Morange, S.; Chitchumroonchokchai, C.; Gleize, B.; Borel, P. The Effect of an Iron Supplement on Lycopene Metabolism and Absorption During Digestion in Healthy Humans. *Mol. Nutr. Food Res.* **2019**, *63*, 1900644.
(43) Grison, S.; Favé, G.; Maillot, M.; Manens, L.; Delissen, O.; Blanchardon, E.; Dublineau, I.; Aigueperse, J.; Bohand, S.; Martin, J.-C.; Souidi, M. Metabolomics reveals dose effects of low-dose chronic exposure to uranium in rats: identification of candidate biomarkers in urine samples. *Metabolomics* **2016**, *12*, 154.
(44) Hyberts, S. G.; Milbradt, A. G.; Wagner, A. B.; Arthanari, H.; Wagner, G. Application of iterative soft thresholding for fast reconstruction of NMR data non-uniformly sampled with multi-dimensional Poisson Gap scheduling. *J. Biomol. NMR* **2012**, *52*, 315−327.
(45) Hyberts, S. G.; Takeuchi, K.; Wagner, G. Poisson-gap sampling and forward maximum entropy reconstruction for enhancing the resolution and sensitivity of protein NMR data. *J. Am. Chem. Soc.* **2010**, *132*, 2145−2147.
(46) Herrera, L. C.; Potvin, M. A.; Melanson, J. E. Quantitative analysis of positional isomers of triacylglycerols via electrospray ionization tandem mass spectrometry of sodiated adducts. *Rapid Commun. Mass Spectrom.* **2010**, *24*, 2745−2752.
(47) Kyle, J. E.; Zhang, X.; Weitz, K. K.; Monroe, M. E.; Ibrahim, Y. M.; Moore, R. J.; Cha, J.; Sun, X.; Lovelace, E. S.; Wagoner, J.; Polyak, S. J.; Metz, T. O.; Dey, S. K.; Smith, R. D.; Burnum-Johnson, K. E.; Baker, E. S. Uncovering biologically significant lipid isomers with liquid chromatography, ion mobility spectrometry and mass spectrometry. *Analyst* **2016**, *141*, 1649−1659.
(48) Wojcik, R.; Webb, I. K.; Deng, L.; Garimella, S. V. B.; Prost, S. A.; Ibrahim, Y. M.; Baker, E. S.; Smith, R. D. Lipid and Glycolipid Isomer Analyses Using Ultra-High Resolution Ion Mobility Spectrometry Separations. *Int. J. Mol. Sci.* **2017**, *18*, 183.
(49) Blase, R. C.; Silveira, J. A.; Gillig, K. J.; Gamage, C. M.; Russell, D. H. Increased ion transmission in IMS: A high resolution, periodic-focusing DC ion guide ion mobility spectrometer. *Int. J. Mass Spectrom.* **2011**, *301*, 166−173.

https://dx.doi.org/10.1021/acs.jproteome.9b00845
J. Proteome Res. 2020, 19, 1674−1683

(50) May, J. C.; McLean, J. A. Ion mobility-mass spectrometry: time-dispersive instrumentation. *Anal. Chem.* **2015**, *87*, 1422−1436.
(51) Thomas, M. C.; Mitchell, T. W.; Harman, D. G.; Deeley, J. M.; Murphy, R. C.; Blanksby, S. J. Elucidation of double bond position in unsaturated lipids by ozone electrospray ionization mass spectrometry. *Anal. Chem.* **2007**, *79*, 5013−5022.
(52) Ma, X.; Chong, L.; Tian, R.; Shi, R.; Hu, T. Y.; Ouyang, Z.; Xia, Y. Identification and quantitation of lipid C=C location isomers: A shotgun lipidomics approach enabled by photochemical reaction. *Proc. Natl. Acad. Sci. U. S. A.* **2016**, *113*, 2573−2578.
(53) Wall, R.; Ross, R. P.; Fitzgerald, G. F.; Stanton, C. Fatty acids from fish: the anti-inflammatory potential of long-chain omega-3 fatty acids. *Nutr. Rev.* **2010**, *68*, 280−289.
(54) Serhan, C. N.; Chiang, N.; Van Dyke, T. E. Resolving inflammation: dual anti-inflammatory and pro-resolution lipid mediators. *Nat. Rev. Immunol.* **2008**, *8*, 349−361.
(55) Innis, S. M. Dietary omega 3 fatty acids and the developing brain. *Brain Res.* **2008**, *1237*, 35−43.

https://dx.doi.org/10.1021/acs.jproteome.9b00845
J. Proteome Res. 2020, 19, 1674−1683